ChemComm

COMMUNICATION

View Article Online
View Journal | View Issue

Cite this: *Chem. Commun.*, 2016, 52, 6825

Received 22nd March 2016,
Accepted 26th April 2016

DOI: 10.1039/c6cc02493a

www.rsc.org/chemcomm

Understanding surface reactivity of Si electrodes in Li-ion batteries by *in operando* scanning electrochemical microscopy†

E. Ventosa,*[a] P. Wilde,[a] A.-H. Zinn,[b] M. Trautmann,[a] A. Ludwig[bc] and W. Schuhmann*[ac]

In operando **SECM is employed to monitor the evolution of the electrically insulating character of a Si electrode surface during (de-)lithiation. The solid–electrolyte interface (SEI) formed on Si electrodes is shown to be intrinsically electrically insulating. However, volume changes upon (de-)lithiation lead to the loss of the protecting character of the initially formed SEI.**

The energy density of state-of-the-art Li-ion batteries (LIBs) does not fulfil the requirements for applications such as pure electric vehicles.[1] Hence, great efforts are directed to the development of high voltage and/or high energy density battery materials. For the negative electrode, Si is among the most promising candidates due to its high energy density, cathodic operating potential as well as its abundance.[2–5] However, Si undergoes extreme volume changes (Si – $Li_{4.4}Si$: 400%) upon (de-)lithiation to accommodate the large amount of stored charge.[2–5] Evidently, this volume change is detrimental for the long-term electrochemical performance of Si electrodes. A comprehensive understanding of the mechanisms involved in (de-)lithiation requires the use of *in situ* techniques. *In situ* microscopes such as transmission electron or atomic force microscopy provide valuable information on Si electrodes for LIBs.[6–11] Recently, scanning electrochemical microscopy (SECM) has been employed for *in situ* investigation of LIB materials.[12–19] Feedback-mode SECM provides laterally resolved information about the electrochemical reactivity of the electrode surface, which is directly related to the electric properties of the SEI. Here, SECM in the feedback mode is employed for the *in operando* investigation of Li (de-)lithiation at Si electrodes.

Amorphous thin film Si (500 nm) was used as a model Si electrode, in which any unwanted influence by binder or particle interaction is avoided. Si particles >150 nm are known to fracture due to the mechanical stress during (de-)lithiation.[20] In contrast, for Si thin films (thickness: several hundred nanometers) the volume change results in the formation of "cracks".[21,22]

In operando optical microscopy was first employed to monitor the formation of these cracks during the first electrochemical (de-)lithiation (Fig. 1a). The formation of cracks became visible in the final stages of delithiation. However, optical microscopy cannot distinguish whether the cracks are formed during delithiation or only become visible during the delithiation as a result of the shrinkage. Fig. 1b shows an atomic force microscopy (AFM) image of the Si electrode after the first complete cycle between 3.00–0.01 V *vs.* Li/Li^+. There are two types of cracks, seen as bright and dark lines. The former are elevated by about 0.1–1 μm above the baseline, while the latter are 500 nm deep, which is the thickness of the Si film (cross sections of Fig. 1b are shown in Fig. S1, ESI†). The bright lines most likely result from the promoted formation of a SEI at the sharp edges of the crack. Since SEI formation is a cathodic process, cracks featured as bright lines can be only explained by cathodic formation, *i.e.*, cracks originate from processes occurring during lithiation. On the other hand, the dark lines correspond to those cracks observed by optical microscopy (Fig. S2, ESI†), which became visible during delithiation. Since SEI formation is a cathodic process, the appearance of cracks during delithiation (anodic) could introduce a discontinuity in the electrically insulating character of the electrode surface allowing more electrolyte decomposition in the subsequent cathodic cycle. Similar to optical microscopy, topography images from AFM cannot confirm whether the cracks are formed or only became visible during the delithiation process. AFM does not provide *in situ* information about the electrically insulating character of the electrode surface. On the other hand, feedback-mode SECM was previously used for studying the electric properties of the SEI in Li-ion batteries.[12,15–19]

[a] *Analytical Chemistry – Center for Electrochemical Sciences (CES), Ruhr-Universität Bochum, D-44780 Bochum, Germany. E-mail: edgar.ventosa@rub.de, wolfgang.schuhmann@rub.de*
[b] *Institute for Materials, Ruhr-University Bochum, Universitätsstraße 150, 44801 Bochum, Germany*
[c] *Materials Research Department, Ruhr-Universität Bochum, Universitätsstr.150, 44780 Bochum, Germany*

† Electronic supplementary information (ESI) available: Details about the sample preparation, the electrochemical cell, the chemicals, the measurements with optical, atomic force and scanning electrochemical microscopy. See DOI: 10.1039/c6cc02493a

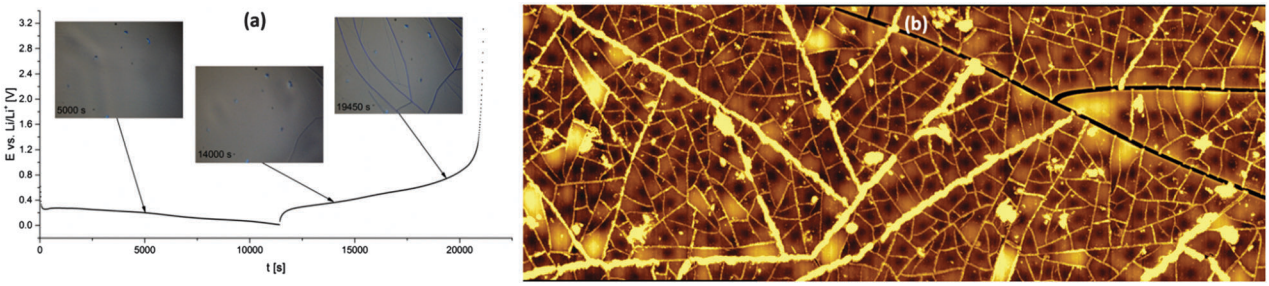

Fig. 1 (a) Potential profile during (de-)lithiation of the Si electrode together with images (1200 × 1600 μm) taken from *in operando* optical microscopy. (b) AFM image (100 × 300 μm) of the Si electrode taken after the first electrochemical cycle. The height scale in the AFM image is 1.12 μm. Cross sections of the AFM images are shown in the ESI.†

SECM can elucidate whether a discontinuity of the local electrochemical activity takes place, and, if so, when and where it occurs. To gather "real-time" information about the changes in the surface reactivity during (de-)lithiation local SECM measurements were carried out. The microelectrode (ME) used as SECM tip does not scan the surface, but it remains at a given position of several micrometres above the Si surface. Fig. 2 shows the current recorded at the Si electrode (black line) together with the feedback current which was simultaneously recorded at the SECM tip (blue line) during the first (Fig. 2a) and second cyclic voltammetric scan (Fig. 2c) at a scan rate of 0.2 mV s^{-1} in 1 M $LiClO_4$ in ethylene carbonate:propylene carbonate (EC:PC). During the experiment the SECM tip was polarized at a constant potential of 3.6 V *vs.* Li/Li^+ at a constant position 12 μm above the Si surface (see ESI† for more details on the SECM experiments). The cyclic voltammograms obtained from the Si electrode (black line) show the typical features of Si electrodes during (de-)lithiation.[2–5,10,11,19–22] The specific charge derived from the anodic peak was 2100 mA h g^{-1} and 2600 mA h g^{-1},respectively, which are comparable to values reported in literature.[4,21,22] The corresponding tip current provides information regarding the charge transfer rate at the surface of the Si electrode. In a simplistic view, values of $I_T/I_{bulk} > 1$ reveal the occurrence of fast charge transfer at the surface of the Si electrode (electrically conducting surface, Fig. 2i), while values <1 indicate hindered charge transfer (electrically insulating surface, Fig. 2ii). Initially, the value of I_T/I_{bulk} was *ca.* 0.8 (blue dot in Fig. 2a) due to the electrically insulating character of native SiO_x on the surface of the Si electrode (Fig. S4, ESI†).[23] Note that the SiO_x layer was not formed during the preparation of the film (see ESI†), but it was spontaneously formed while stored outside the glovebox at room temperature. Consequently, this SiO_x layer is expected to be ultrathin. I_T/I_{bulk} increased in the negative-going scan due to the increased driving force at the Si electrode for the regeneration of the free-diffusing redox species. I_T/I_{bulk} at the tip reached a value of 1.25–1.30 at 2.0 V *vs.* Li/Li^+ and remained stable. These values for I_T/I_{bulk} above 1 confirm that the SiO_x layer is very thin since positive feedback would not be possible for complete passivating thicker SiO_x layer. The I_T/I_{bulk} value was expected to remain constant if the electric properties of the electrode surface did not change, but it drastically dropped when potentials more cathodic than 0.5 V *vs.* Li/Li^+ were applied to the Si electrode. I_T/I_{bulk} continued decreasing until the end of the negative-going scan at 0.01 V *vs.* Li/Li^+. During the positive-going scan, the value of I_T/I_{bulk} continued decreasing until an applied potential of 0.6 V *vs.* Li/Li^+. This further decrease in the SECM tip current observed during the positive-going scan is due to the still sufficiently high cathodic potentials to lithiate Si and to form the SEI. Note that a cathodic current through the Si electrode was observed during the positive-going scan in the potential range from 0.01 to 0.2 V. Moreover, the release of Li^+ from the sample introduces migration effects, which were previously suggested to decrease the signal at the SECM tip.[15,24] The most interesting feature occurred at 0.7 V *vs.* Li/Li^+ during the positive-going scan, where a drastic increase in the tip current was observed. I_T/I_{bulk} values changed from negative to positive feedback, revealing the loss of the electric insulating character of the SEI covered Si electrode. In fact, the I_T/I_{bulk} value at the end of the first cycle (*ca.* 1) was higher than that recorded at the same potential (3.0 V) before the voltammogram (*ca.* 0.75). Considering that the surface of the Si electrode is covered not only by ultrathin SiO_x but also by the SEI, the higher I_T/I_{bulk} after the first cycle indicates discontinuities in the SEI and ultrathin SiO_x films, which allow faster regeneration of the redox species. Since the fracture of ultrathin SiO_x is an irreversible process that occurs during the first lithiation, the discontinuity in the ultrathin SiO_x thin film at the end of the first cycle was not surprising. However, the discontinuity in the SEI at the end of the first cycle was not anticipated assuming cathodic formation of the cracks. If fractures occurred during the volume expansion during lithiation (cathodic), they should immediately self-heal since the potentials are still very cathodic (<0.3 V). The discontinuity in the SEI at the end of the first cycle revealed by SECM indicates that the electrolyte continues decomposing and forming the SEI during the second lithiation, regardless whether new fractures are formed. The current recorded at the Si electrode (black line) as well as at the tip (blue line) followed a similar trend in the second cycle (Fig. 2c). The electrode surface became electrically insulating at cathodic potentials. The migration effects of Li^+ uptake and release from the Si electrode in the signal of the tip (bumps) did not allow a precise determination of the potential at which the change in the electrically insulating character occurred. Importantly, I_T/I_{bulk} values remained <0.75 during the entire positive-going scan, which demonstrates that new discontinuities in the SEI did not occur during the second anodic cycle.

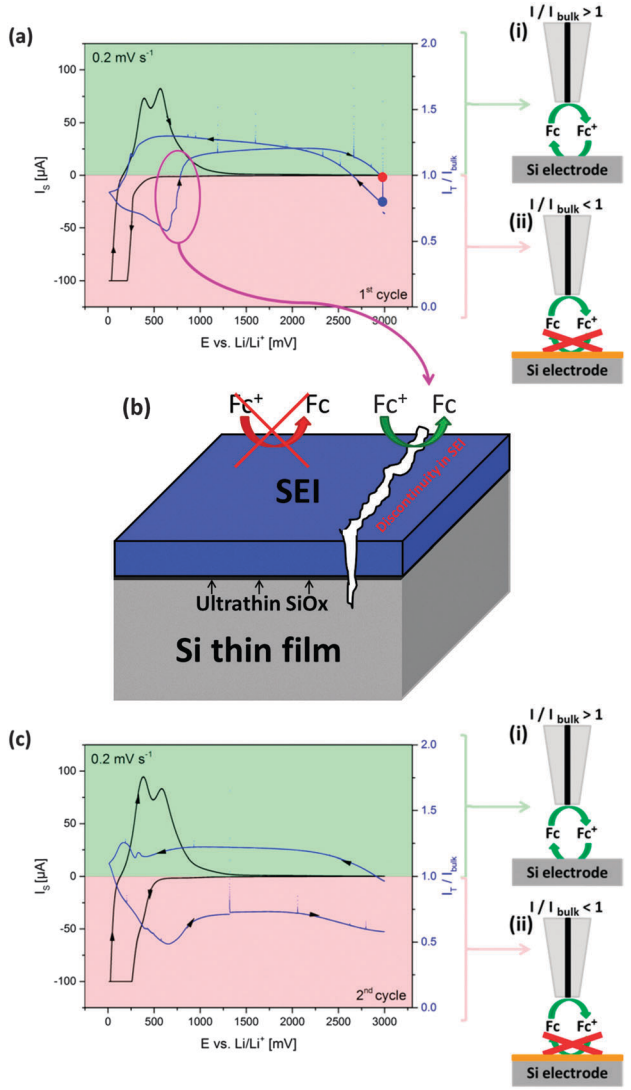

Fig. 2 *In operando* SECM measurements of the (a) first and (c) second cycle, showing a cyclic voltammogram at the Si electrode at a scan rate of 0.2 mV s^{-1} (black line) in 1 M $LiPF_6$ in 1 : 1 EC : DEC, and the normalized feedback current (blue line) recorded at the Pt tip positioned at 12 µm above the sample. The potential applied to the Pt tip was 3.6 V *vs.* Li/Li^+. Insets (i) and (ii) are schematic representations of positive feedback and negative feedback, respectively. (b) Schematic of the formation of a discontinuity in the SEI and SiO_x and its effect on the feedback current recorded at the SECM tip.

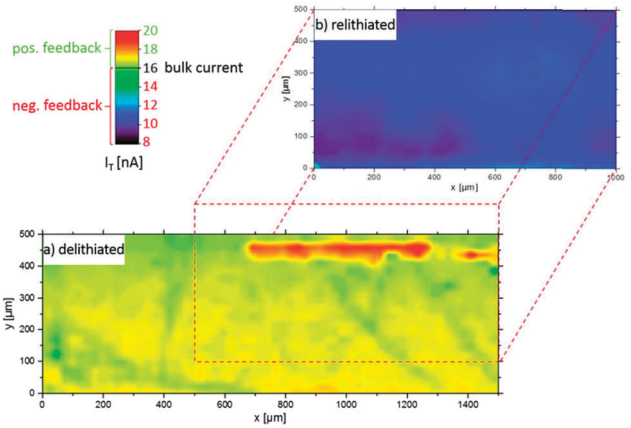

Fig. 3 *In situ* SECM mapping of the Si electrode (a) after the first delithiation (3 V *vs.* Li/Li^+) and (b) after the second lithiation (0.016 V *vs.* Li/Li^+). I_T values above and below 16 nA correspond to positive and negative feedback (electrically conducting and insulating), respectively.

In operando optical microscopy (Fig. 1a) showed the appearance of cracks during the first delithiation. If these cracks did not only become visible but were indeed formed during delithiation, they should be "SEI-free" and a positive feedback at a tip located above one of these cracks should be expected. Since *in operando* SECM measurements must be carried out at a single location above the Si electrode surface, there is a certain possibility that the tip was located above one of these cracks. To gain spatially resolved information about the electrically insulating character of the entire surface area, *in situ* SECM maps were taken after the first delithiation and after the second lithiation (Fig. 3). Note that the positive and negative feedback in Fig. 3 corresponds to colours ranging from green to red and green to dark blue, respectively. The image taken at 3.0 V *vs.* Li/Li^+ after the first delithiation (Fig. 3a) revealed two important points. The large cracks formed during the first delithiation and observed by *in operando* optical microscopy were also visible in the SECM image, seen as a red stripe in the upper-right area of the image. In this region, the positive I_T/I_{bulk} values of *ca.* 1.3 indicate a clear discontinuity in the SEI. Most of the scanned area displayed a slightly positive feedback (*ca.* 1.05) giving rise to a distinct yellowish tone in the overall image. In the SECM measurement (Fig. 2), the I_T/I_{bulk} value recorded after the first delithiation was *ca.* 1 red dot in Fig. 2a, which is in good agreement with the average I_T/I_{bulk} value of the entire sample (Fig. 3). Therefore, *in operando* SECM results shown in Fig. 2 do not represent the single behaviour of a non-representative point but the general behaviour of most of the surface area. After the first cycle, the potential of the sample was scanned cathodically down to 0.01 V *vs.* Li/Li^+, and a SECM image was recorded at a potential of 0.016 V after the second lithiation (Fig. 3b). This image confirmed that the red stripe (positive feedback) observed in the upper-right area at 3.0 V *vs.* Li/Li^+ was not a topography-feature since it disappeared at 0.016 V *vs.* Li/Li^+. Moreover, the entire electrode surface became electrically insulating with an average I_T/I_{bulk} value of *ca.* 0.7. The discontinuities in the SEI, which were formed during the first delithiation due to the mechanical stress, were "healed" during the second lithiation. As a result, the "protecting" character provided by a continuous SEI was regained over the entire Si electrode after the second lithiation. This observation together with *in operando* SECM measurements demonstrate that the SEI formed at the Si electrode possesses the necessary electrically insulating character, and the volume changes during (de-)lithiation are responsible for the loss in the "protecting" character at the electrode surface.

In conclusion, the evolution of the electrically insulating character of the Si electrode surface was investigated for the first time by *in operando* SECM, using a thin film Si electrode as a model sample. With the assistance of *in operando* optical microscopy and AFM, SECM measurements indicate that two types of cracks are

formed during the first cycle, namely cracks partially covered by SEI and SEI-free cracks. Obviously, the latter introduces a discontinuity in the electrically insulating character of the electrode surface, which leads to the decomposition of electrolyte solution in the second cycle. Surprisingly, most of the electrode surface lacks the electrically insulating character that a SEI is supposed to provide after the first cycle. *In operando* SECM measurements confirm that the SEI formed on the Si electrode possesses the required electrically insulating character. The volume changes occurring during (de-)lithiation are responsible for the loss in the "protecting" character of the SEI at the electrode surface.

The authors are grateful to the Deutsche Forschungsgemeinschaft (DFG) in the framework of the Cluster of Excellence "Resolv" (ECX 1069).

References

1 F. T. Wagner, B. Lakshmanan and M. F. Mathias, *J. Phys. Chem. Lett.*, 2010, **1**, 2204.
2 M. N. Obrovac and V. L. Chevrier, *Chem. Rev.*, 2014, **114**, 11444.
3 X. Su, Q. Wu, J. Li, X. Xiao, A. Lott, W. Lu, B. W. Sheldon and J. Wu, *Adv. Energy Mater.*, 2014, **4**, 1300882.
4 C. M. Park, J. H. Kim, H. Kim and H. J. Sohn, *Chem. Soc. Rev.*, 2010, **39**, 3115.
5 H. Wu, G. Chan, J. W. Choi, I. Ryu, Y. Yao, M. T. McDowell, S. W. Lee, A. Jackson, Y. Yang, L. Hu and Y. Cui, *Nat. Nanotechnol.*, 2012, **7**, 310.
6 X. H. Liu and J. Y. Huang, *Energy Environ. Sci.*, 2011, **4**, 3844.
7 H. Ghassemi, M. Au, N. Chen, P. A. Heiden and R. S. Yassar, *ACS Nano*, 2011, **5**, 7805.
8 X. H. Liu, Y. Liu, A. Kushima, S. Zhang, T. Zhu, J. Li and J. Y. Huang, *Adv. Energy Mater.*, 2012, **2**, 722.
9 V. Kuznetsov, A. H. Zinn, G. Zampardi, S. Borhani-Haghighi, F. La Mantia, A. Ludwig, W. Schuhmann and E. Ventosa, *ACS Appl. Mater. Interfaces*, 2015, **7**, 23554.
10 A. Tokranov, B. W. Sheldon, C. Li, S. Minne and X. Xiao, *ACS Appl. Mater. Interfaces*, 2014, **6**, 6672.
11 X. Liu, X. Deng, R. Liu, H. Yan, Y. Guo, D. Wang and L. Wan, *ACS Appl. Mater. Interfaces*, 2014, **6**, 20317.
12 E. Ventosa and W. Schuhmann, *Phys. Chem. Chem. Phys.*, 2015, **17**, 28441.
13 A. L. Lipson, R. S. Ginder and M. C. Hersam, *Adv. Mater.*, 2011, **23**, 5613.
14 T. Takahashi, A. Kumatani, H. Munakata, H. Inomata, K. Ito, K. Ino, H. Shiku, P. R. Unwin, Y. E. Korchev, K. Kanamura and T. Matsue, *Nat. Commun.*, 2014, **5**, 5450.
15 G. Zampardi, E. Ventosa, F. La Mantia and W. Schuhmann, *Chem. Commun.*, 2013, **49**, 9347.
16 H. Bülter, F. Peters, J. Schwenzel and G. Wittstock, *Angew. Chem., Int. Ed.*, 2014, **53**, 10531.
17 G. Zampardi, S. Klink, V. Kuznetsov, T. Erichsen, A. Maljusch, F. La Mantia, W. Schuhmann and E. Ventosa, *ChemElectroChem*, 2015, **2**, 1607.
18 E. Ventosa, G. Zampardi, C. Flox, F. La Mantia, W. Schuhmann and J. R. Morante, *Chem. Commun.*, 2015, **51**, 14973.
19 H. Bülter, F. Peters, J. Schwenzel and G. Wittstock, *J. Electrochem. Soc.*, 2015, **162**, A7024.
20 X. H. Liu, L. Zhong, S. Huang, S. X. Mao, T. Zhu and J. Y. Huang, *ACS Nano*, 2012, **6**, 1522.
21 A. H. Zinn, S. Borhani-Haghighi, E. Ventosa, J. Pfetzing-Micklich, N. Wieczorek, W. Schuhmann and A. Ludwig, *Phys. Status Solidi A*, 2014, **211**, 2650.
22 J. Li, A. K. Dozier, Y. Li, F. Yang and Y. T. Cheng, *J. Electrochem. Soc.*, 2011, **158**, A689.
23 H. Bülter, M. Sternad, E. d. Santos Sardinha, J. Witt, C. Dosche, M. Wilkening and G. Wittstock, *J. Electrochem. Soc.*, 2016, **163**, A504.
24 G. Zampardi, E. Ventosa, F. La Mantia and W. Schuhmann, *Electroanalysis*, 2015, **27**, 1017.